Journal Name

ARTICLE

In between molecules and self-assembled fibrillar networks: Highly stable nanogel particles from a low molecular weight hydrogelator

Received 00th January 20xx,
Accepted 00th January 20xx

DOI: 10.1039/x0xx00000x

www.rsc.org/

Ana Torres-Martínez, César A. Angulo-Pachón, Francisco Galindo* and Juan F. Miravet*

The preparation of molecular, non-polymeric, nanogels from a low molecular weight hydrogelator is reported. Molecular nanogels are expected to overcome issues associated with the use of polymeric nanogels in biomedicine such as biodegradability, stimuli responsiveness, polydispersity, and batch-to-batch reproducibility. Nanogels formed by compound **1** were reproducibly prepared by sonication of a xerogel in PBS, with a total concentration of *ca.* 2 mM. Intensity averaged diameter of *ca.* 200 nm was determined by DLS. Electron microscopy (TEM and cryo-TEM) revealed spherical particles. Light scattering (SALS) indicates that water is the main component of the nanoparticles, being the concentration of **1** in the nanogels of *ca.* 3 mg/mL. These particles can be considered to constitute an intermediate state between free molecules and self-assembled fibrillar networks. The nanogels present excellent temporal and thermal stability and accessible hydrophobic domains, as demonstrated by the incorporation of the fluorescent dye Nile Red.

Introduction

Organic nanoparticles have been increasingly studied as vehicles for the delivery of actives in a biomedical context.[1] Examples include liposomes,[2, 3] solid-lipid nanoparticles,[4] polymeric nanoparticles[5] and dendrimers.[6] Incorporation of bioactive species into nanocarriers addresses issues such as low solubility, intrinsic chemical instability, opsonization or rapid clearance.[7] Furthermore, studies aim to find specific biodistribution with the help of nanosized structures, based on the different permeability of tissues or stimuli-responsive containers.[8] As a matter of fact, a few tens of nanoparticle-based medicines have been approved by FDA.[9]

Nanogels are a particular group of organic nanostructures which lately has received much attention as carriers due to their advantages over other nanoparticles, like improved flexibility and biocompatibility.[10-20] The use of nanogels as vehicles is inspired by their macroscopic counterparts, which have been extensively studied in controlled release.[21, 22] In the literature, nanogels (nanohydrogels) are described as nanoparticles formed by three-dimensional polymeric networks capable of retaining large quantities of water. Different preparation procedures have been reported.[23] Most of the described nanogels are constituted by covalently crosslinked networks, formed, for example, by emulsion polymerization,[24] following the seminal work of Vinogradov with poly(ethylene glycol)-polyethyleneimine particles.[25, 26] Alternatively, nanogels can be prepared from polymer precursors, which are crosslinked with labile groups to improve biodegradability and stimuli responsiveness.[27] Physically crosslinked nanogels have been reported based, for example, in the self-assembly of amphiphilic block copolymers[28], hydrophobized polysaccharides[29] or DNA.[30]

In opposition to polymeric gels, molecular gels (also named supramolecular gels) are formed by low molecular weight molecules and their study has blossomed in the last two decades.[31-37] These gels are formed by 1-D anisotropic molecular aggregation, resulting in self-assembled fibrillar networks. Distinctly from polymeric gels, the fibres are fully reversible, yielding the original free molecules upon changes of temperature or other physicochemical stimuli.[38] Areas such as controlled release, catalysis, tissue engineering or optoelectronics, among others, have been attracted by these materials. In particular, special interest has grown regarding molecular hydrogels in a biomedical context.[36]

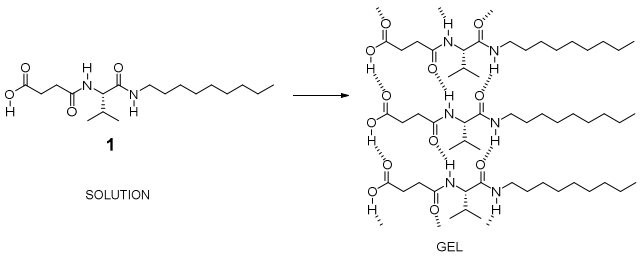

Scheme 1. Structure of compound **1** and proposed aggregation model.

[a] *Departament de Química Inorgànica i Orgànica, Universitat Jaume I, Avda. Sos Baynat s/n, 12071 Castelló, Spain.*

Electronic Supplementary Information (ESI) available: NMR spectra, mgc values in different solvents, data from potentiometric titration, DLS correlogram, SALS Debye plot for polystyrene latex and calculation of the concentration of **1** in the form of nanoparticles.

The preparation of molecular nanogels represents an exciting challenge taking into account their envisaged unique properties in comparison with polymeric analogues. Some critical issues in the use of polymeric nanogels such as biodegradability, stimuli responsiveness, polymer polydispersity, and batch-to-batch reproducibility are intrinsically solved in molecular gels. Here, we report the formation of stable nanogel particles of compound **1** (Scheme 1), a molecular hydrogelator. This work follows our initial efforts on this direction, which afforded nanoparticles from a molecular gelator derived from naphthalimide.[39] In that case, the nature of the nanoparticles, solid or gel-like, could not be clarified, and the particles showed poor stability towards aggregation at concentrations above *ca.* 20 μM. Up to our knowledge, the present work constitutes the first report on the preparation and detailed characterization of molecular nanogels.

Results and discussion

Compound **1** (Scheme 1) consists of an L-valine unit modified as a nonylamide at the carboxylic acid unit and acylated with succinic acid at the amine function. In previous work of our group, related amphiphilic structures with variations of the aliphatic chain length or the amino acid unit have been shown to form pH-responsive hydrogels. The aggregation in water of this type of molecules should be based in hydrophobic forces complemented with multiple H-bonds as reported for related systems.[40] A tentative aggregation model is shown in Scheme **1,** based in those proposed for closely related molecules previously described.[41, 42]

Gels of **1** could be formed in water by cooling down hot solutions of the gelator, with a minimum gelation concentration value (*mgc*) of 5 mg mL^{-1} (16 mM). Additionally, gels can also be prepared in different organic solvents with *mgc* in the range 3-38 mM (see ESI). Transmission electron microscopy images of the xerogel from water and toluene (Figure 1) revealed a fibrillar structure, as commonly described for molecular gels. Noticeably the fibers in the xerogel from water are straight and monodisperse, with a diameter of *ca.* 20 nm, while those obtained in toluene show more flexibility, being curved and entangled. These morphological differences probably reflect the different arrangement of the gelator molecules in the fibers, being hydrophobic forces dominant for the aggregation in water and polar interactions, namely hydrogen bonding, predominant in organic solvents. Indeed, differential scanning microscopy reveals that the water and toluene xerogels are polymorphic, presenting different melting points and endothermic polymorphic transitions (see ESI).

The presence of an ionizable carboxylic unit in **1** results in pH-dependent gelation properties. Potentiometric titrations were carried out to evaluate the pH range of existence of neutral species of **1**, revealing an apparent pKa of 7.6 (see ESI). As has been previously reported, this pKa value is considerably shifted when compared to soluble, non-aggregating carboxylic acids, which present pKa values around 3-5.[43-45] The reduced acidity of **1** could be ascribed to the thermodynamic stabilisation of neutral species gained from the aggregation process.

Following a report on the formation of hybrid peptide-quantum dots colloidal spheres,[46] nanogel particles were prepared by sonication of a xerogel of **1** suspended in aqueous medium. For this purpose, a gel was prepared in toluene, and the corresponding xerogel was obtained by solvent evaporation under vacuum. Upon sonication in phosphate buffer saline (PBS, 10 mM, pH=7), a colloidal suspension of the nanoparticles with a final pH of 6.4 was obtained. Centrifugation to remove large fragments of the xerogel particles afforded an optically clear suspension of the nanogels, which was analysed by dynamic light scattering (DLS).

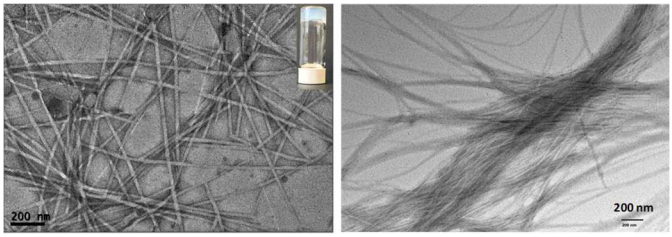

Figure 1. TEM image of the xerogels obtained from **1** in water (left) and toluene (right). Inset: the macroscopic aspect of the hydrogel.

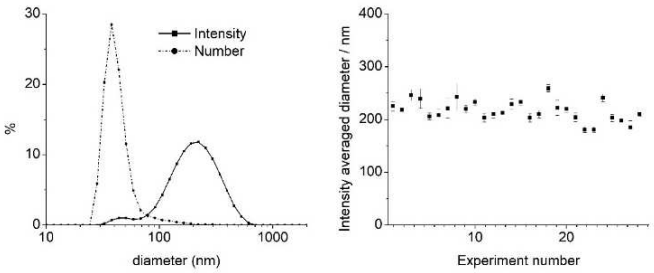

Figure 2. Left: Size distribution by intensity (solid line) and by number (dash-dot line) of a representative sample of nanogel particles obtained by DLS analysis. Right: Intensity averaged diameter of 29 different nanogels samples.

As can be seen in Figure 2, a bimodal distribution of intensity averaged diameters (D_i) with maxima at *ca.* 200 and 50 nm was obtained (examine correlogram at ESI). The conversion of these data to number averaged diameters (D_n) shows that particles with a diameter around 50 nm are predominant. The procedure for the preparation of the nanoparticles was found to be quite reproducible, and a set of 29 preparations afforded similar results, as reflected in Figure 2.

The efficiency of the transformation of the xerogel into nanoparticles was evaluated determining the concentration of **1** in the colloids by ^{1}H NMR. For this purpose, the signals were integrated using a calibrated electronic signal (ERETIC).[47] The concentration of nanogel particles was found to be reproducible. For a set of 10 experiments, using an initial concentration of xerogel of 1.2 mg mL^{-1}, an average concentration of **1** in the sample of 0.71 $\pm$ 0.14 mg mL^{-1}, namely, 2.1 $\pm$ 0.4 mM, was obtained.

The same procedure was assayed for the xerogel obtained from an aqueous medium, and again particles with similar size distribution were obtained (see ESI). These results highlight that

the solvent from which the xerogel is obtained is not, a priori, a key parameter in the preparation of the nanoparticles. However, sonication of finely powered solid gelator did not permit to get the nanoparticles, revealing that the high surface ratio of the fibrillar xerogels is essential for their transformation into nanogels. It was decided to focus on the study of the particles obtained from the toluene xerogel because, for future envisaged studies, the use of an organic solvent should be favourable for the entrapment of actives which are poorly soluble in water.

Unlike *mgc*, which determines the amount of compound required to form a sample spanning network, the critical aggregation concentration, *cac*, indicates the onset of self-assembly and represents the dilution limit for thermodynamically stable aggregates. Determination of *cac* in acidic medium for **1** was carried out using pyrene as a fluorescent probe. The incorporation of pyrene into hydrophobic environments leads to an increase of intensity of its emission band III (see Figure 3).[48] Fluorescence spectra were recorded for samples with increasing concentrations of **1**.

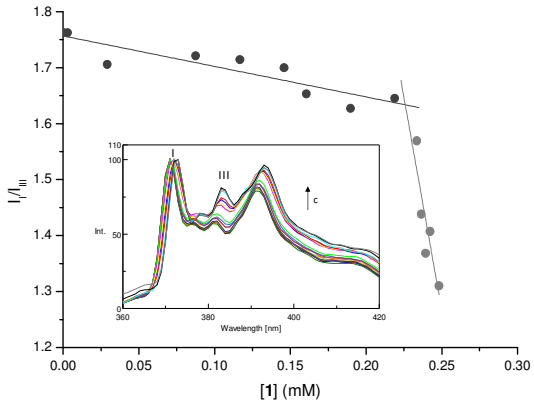

Figure 3. Variation of the relative intensity of emission bands I and III of pyrene in the presence of increasing concentrations of compound **1** in water. λ_{exc}= 334 nm

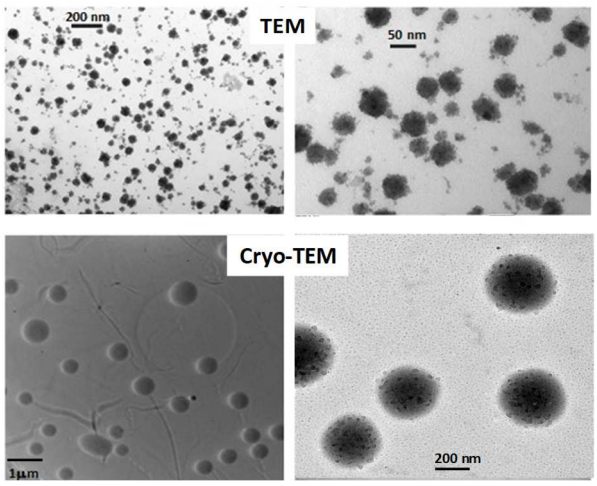

Figure 4. Electron microscopy images of nanogels particles formed by **1.**

As can be seen in Figure 3, the measured fluorescence ratio shows a moderate decrease with concentration up to a point where a dramatic tendency change is observed, with much steeper slope, resulting in a *cac* value of 0.22 mM.

Transmission electron microscopy (TEM) analysis revealed the presence of irregular spherical objects with diameters around 50 nm (Figure 4, top). The particles were also observed by cryo-TEM (Figure 4, bottom), revealing diameters of *ca.* 200 nm. Cryo-TEM images suggest a sponge-like structure with dark dots that might correspond to non-vitreous water trapped inside the particles.[49] The smaller particle diameter observed by TEM when compared to Cryo-TEM could be ascribed to drying effects associated with the former technique.

To evaluate the gel-like nature of the nanoparticles, an average concentration of **1** within the particle ($[\mathbf{1}]_{NP}$) can be calculated from equation *(1)*, being M_w the apparent molecular weight of the particle, r the radius of the particle and N_A Avogadro's number.[29, 50, 51, 52]

$$[\mathbf{1}]_{NP} = M_w/N_A\ (4/3\ \pi r^3)^{-1} \qquad (1)$$

M_w was obtained by single angle static light scattering (SALS) measurements performed with the DLS equipment available in our laboratories.[53] Light scattering intensity was measured at different concentrations and analysed with the Debye-Zimm relation (see equation *(2)*).[54] In equation *(2), K* is an experimental constant (see equation *(3))* that depends on the wavelength of the incident light (λ_0), the refractive index of the solvent (n_0) and the variation of refractive index with particle concentration (*dn/dc*). Additionally, *c* is sample concentration, R_θ is the ratio of scattered light to incident light, A_2 is the thermodynamic 2nd virial nonideality coefficient, and $P(\theta)$ is the angular dependence of scattering intensity.

$$K\ c/R_\theta = (1/M_w + 2\ A_2\ c)\ P(\theta) \qquad (2)$$

$$K = (4\ \pi^2/\lambda_0 4\ N_A)\ (n_0\ dn/dc)^2 \qquad (3)$$

For the study of the nanogels of **1,** *dn/dc* was found to be 0.063 mL g^{-1} and scattering of four samples with different concentrations was measured (Table 1). It has to be noted that given the supramolecular nature of the nanoparticles and their pH-sensitivity, the concentration of **1** in the form of nanoparticles should be less than the total amount of **1** in the sample. The presence of the ionised compound, pKa = 7.6, and free **1** corresponding to the *cac* value are considered (see ESI). Graphical representation of the value $K\ c/R_\theta$ vs. *c* affords the so-called Debye plot, being the intercept of the linear fitting at *c* = 0 the value of $1/M_w$ (Figure 5). A good correlation was obtained, and the apparent M_w was calculated to be 13.8 10^6 ± 8.3 10^6 Da (see details of error estimation in the Methods section). Using this value and the diameter obtained by DLS for the studied samples (210 nm), an average concentration of **1** in the particles of 4.7 ± 2.8 mg mL^{-1} is calculated with equation *(1).* This result reveals the gel-like nature of the nanoparticles, being water the main component. The concentration of **1** in the particles is similar to that described for polyethylene glycol with M_W = 2 10^6 Da, 2.9 mg mL^{-1},[55] and comparable to that found, for example,

in microgels[50, 56] or pullulan nanogels,[52, 57] which show a polymer concentration in the range 10-30 mg mL^{-1}.

Table 1. Light scattering intensity obtained for aqueous dispersions of nanoparticles of **1** at different concentrations.

[**1**] / mg mL^{-1}	Count rate / kcps	$10^4\ K\ c\ R_\theta^{-1}$ / kDa^{-1}
0.54	1058	1.36
0.45	922	1.30
0.36	781	1.24
0.27	654	1.11
0.17	527	0.88

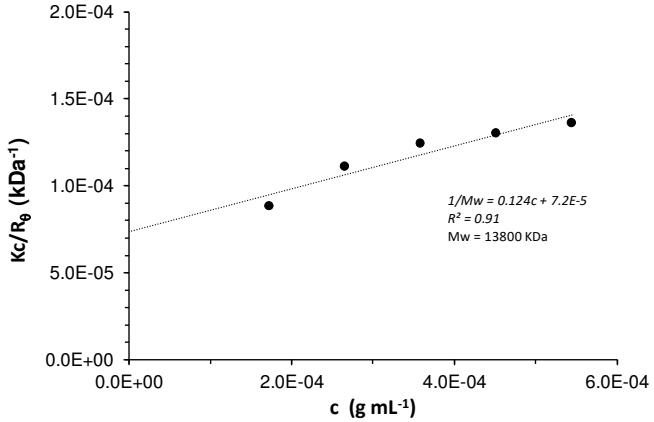

Figure 5. Debye plot obtained for the SALS study of the nanoparticles.

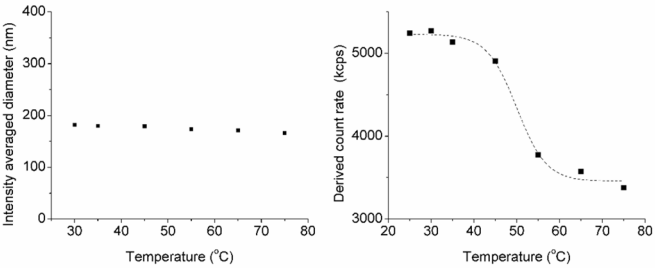

Figure 6. Influence of temperature in the size of the nanogels (left) and in the intensity of scattered light (right).

The average concentration of gelator in the particles is closely related to the so-called overlap concentration, which is used in polymer chemistry and is defined as the point where the concentration within a given polymer particle is equal to the solution concentration.[58] By analogy, $[\mathbf{1}]_{NP}$ would represent the total sample concentration required for the onset of interparticle interactions, leading to gelation. Notably, there is a reasonable agreement between $[\mathbf{1}]_{NP}$, 4.7 $\pm$ 2.8 mg mL^{-1}, and *mgc*, 5 mg mL^{-1}.

The TEM images commented above do not permit to distinguish a fibrillar structure within the particles, such as that observed in the parent macroscopic gels. Indeed, it does not seem feasible the formation of such small nanoparticles by fibers of width as such found in the xerogels. Consequently, the sonication, rather than fracturing the xerogel fibers, should provoke solubilisation of the monomers, affording local concentrations high enough to form seminal fibrils, which are described as precursors of fibers in the formation of macroscopic gels. [59] The gel-like nature of the particles should be ascribed to the entanglement of those seminal fibrils into spherical particles. Therefore, the nanogel particles would correspond to the initial stages of the aggregation of molecular gels, and constitute an intermediate state between free molecules and fibrillar objects. On this regard, kinetic studies usually find that molecular gels are formed by a nucleation-growth mechanism,[45, 60, 61] and it was recently reported that fibres could be formed by scrolling of supramolecular lamellae that present asymmetric surfaces.[62]

The nanogels presented good temporal stability. Similar DLS results were obtained when stored at room temperature for 4 days. Samples stored at 4 ^{o}C were stable after ten days. The Z-potential of the particles was measured to be of -65 mV, a value in the range of those reported for highly stable colloids.[63] The particles are stable upon dilution with PBS in the concentration range 0.25-2 mM, with no diameter variation (see ESI). Stability towards temperature between 30 and 75 ^{o}C was also assayed by DLS. As shown in Figure 6, the intensity averaged diameter was not affected by temperature changes but, on the other hand, the intensity of scattered light dropped significantly at 50 ^{o}C, suggesting partial solubilisation of **1**.

The results abovementioned about the determination of *cac* demonstrate that the initial aggregates formed upon increasing concentration of **1** can entrap hydrophobic species such as pyrene, but no nanogel preparation was carried out in that study. To test the accessibility of the hydrophobic domains of the nanogel particles, experiments using the fluorescent dye Nile Red were carried out. Nile Red is almost nonfluorescent in water and other polar solvents but displays intense fluorescence emission in nonpolar environments.

Additionally, the emission maximum of this probe is strongly affected by the polarity of the medium, changing dramatically from 666 nm in water to 606 nm in dichloromethane and 570 nm in cyclohexane.[64] As can be seen in Figure 7, when nanogels were prepared in the presence of the dye a notable increase in fluorescence was observed compared with a control in the absence of nanogels. The emission maximum of Nile Red @ **1** is shifted to 587 nm, indicating a quite hydrophobic environment.

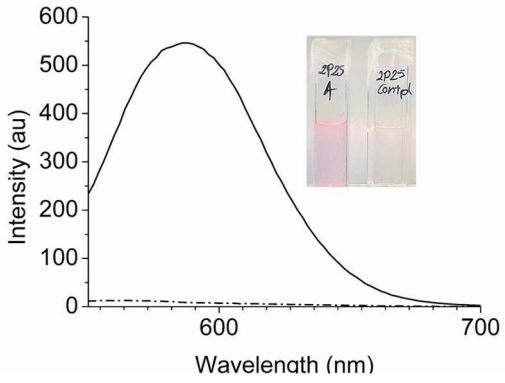

Figure 7. Representative fluorescence emission spectra of Nile Red@**1** (solid line) and the free dye (dash-dot line). [Nile Red] = 10 μM. Inset: cuvettes containing nanogel particles loaded with Nile Red (left) and free Nile Red (right).

Therefore, these results highlight the presence of accessible hydrophobic domains in the nanogel particles, demonstrating

their potential use for the entrapment of poorly soluble organic actives.

Methods

Synthesis and characterization of 1

The synthesis of **1** is outlined in Scheme 2. Reactions which required an inert atmosphere were carried out under N_2. Commercially available reagents and HPLC grade solvents were used as received.

^{1}H-NMR and ^{13}C-NMR spectra were recorded on Agilent VNMR System spectrometer (500 MHz for ^{1}H-NMR, 125 MHz ^{13}C-NMR) or Bruker Avance III HD spectrometers (400 MHz and 300 MHz for ^{1}H-NMR, 101 MHz and 75 MHz for ^{13}C-NMR) in the indicated solvent at 30 °C. Signals of the deuterated solvent (DMSO-*d6*) were taken as the reference, the singlet at δ 2.50 and the quadruplet centred at 39.52 ppm for ^{1}H and ^{13}C, respectively. ^{1}H-NMR chemical shifts (δ_H) and ^{13}C-NMR chemical shifts (δ_C) are quoted in parts per million (ppm) downfield from trimethylsilane (TMS) and coupling constants (*J*) are quoted in Hertz (Hz). Abbreviations for NMR data are s (singlet), d (doublet), t (triplet), q (quartet), quin (quintet) and m (multiplet). ^{1}H and ^{13}C signals were assigned with the aid of 2D methods (COSY, HSQC and HMBC). Data were processed with the software Mestrenova.

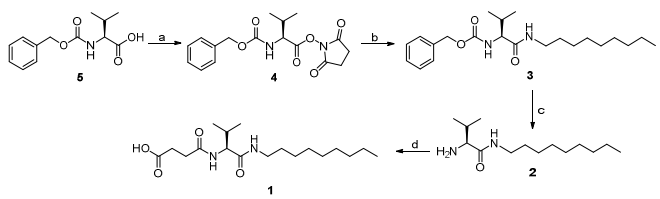

Scheme 2. Preparation of **1**: a) DCC, *N*-Hydroxisuccinimide, THF, 2 h, 94%; b) *n*-Nonylamine, THF, 5 h, 77%; c) Pd/C, H_2, CH_3OH, 4 h, 94%; d) Succinic anhydride, K_2CO_3, THF, 16 h, 97%.

Mass spectra were run by the electrospray mode (ESMS) and were recorded with a Mass Spectrometry triple Quadrupole Q-TOF Premier (Waters) with simultaneous Electrospray and APCI Probe.

(S)-2, 5-dioxopyrrolidin-1-yl 2-(((benzyloxy)carbonyl)amino)-3-methylbutanoate (4): A solution of N-Carbobenzyloxy-*L*-valine **5** (10 g, 40 mmol) and *N*-Hydroxysuccinimide (4.61 g, 40 mmol, 1.0 eq.) in THF (200 mL) was added dropwise under N_2 at 0 °C to a solution of *N*,*N*′-Dicyclohexylcarbodiimide (8.33 g, 40.4 mmol, 1.01 eq.) in THF (100 mL). The mixture was further stirred for 2 h at 0 °C. The solution was then allowed to stand into the refrigerator at 4 °C for 16 h, which caused precipitation of *N*,*N*′-Dicyclohexylurea. Then the mixture was filtered under vacuum, the solvent removed under reduced pressure and the crude residue was purified by crystallization in isopropanol to yield **4** (13.1 g, 37.6 mmol, 94%) as a white solid. The NMR spectra were consistent with those described in the literature.[65]

Benzyl (S)-(3-methyl-1-(nonylamino)-1-oxobutan-2-yl)carbamate (3): A solution of compound **4** (7.58 g, 20 mmol) in THF (90 mL) was added dropwise under N_2 at 25 °C to a solution of *n*-Nonylamine (4.1 mL, 22.8 mmol, 1.1 eq.) in THF (55 mL). The mixture was further stirred for 5 h at 50 °C. The white solid obtained was filtered under vacuum and washed with HCl 0.1 M (100 mL) and water (200 mL). The compound was dried under reduced pressure at 50 °C to yield **3** (5.8 g, 15.4 mmol, 77%) as a white solid. ^{1}H NMR (300 MHz, DMSO-d_6): δ 7.82 (dd, *J* = 5.2, 5.4 Hz, 1H), 7.42 – 7.24 (m, 5H), 7.15 (d, *J* = 8.9 Hz, 1H), 5.02 (s, 2H), 3.78 (dd, *J* = 7.5, 6.6 Hz, 1H), 3.19 – 2.88 (m, 2H), 1.92 (m, 1H), 1.37 (m, 2H), 1.23 (m, 12H), 0.85 (m, 9H). ^{13}C NMR (75 MHz, DMSO-d_6): δ 170.8 (C=O), 156.0 (C=O), 137.1 (C), 128.2 (2xCH), 127.7 (CH), 127.5 (2xCH), 65.3 (CH_2), 60.3 (CH), 38.3 (CH_2), 31.2(CH_2), 30.2 (CH), 28.9 (CH_2), 28.9 (CH_2), 28.7(CH_2), 28.6 (CH_2), 26.3 (CH_2), 22.0 (CH_2), 19.1 (CH_3), 18.2 (CH_3), 13.9 (CH_3). HRMS (ESI-TOF): *m/z* calcd. for $[C_{22}H_{37}N_2O_3]^+$: 377.2804; found: 377.2802 [*M* + H]$^+$ (Δ = 0.3 ppm).

(S)-2-amino-3-methyl-N-nonylbutanamide (2): Palladium catalyst (10% w/w Pd/C, 580 mg) and compound **3**, (5.8 g, 15.4 mmol) were suspended in CH_3OH (350 mL) and stirred under N_2 at room temperature for 10 min. Subsequently, the system was kept under low vacuum and then filled with hydrogen from a latex balloon. Then the mixture was stirred at room temperature for 4 h. After this time Pd/C was removed by filtration through Celite, and the solvent was removed under reduced pressure to yield **2** (3.54 g, 14.6 mmol, 94%) as white solid. The compound was used without further purification for the next reaction. ^{1}H NMR (500 MHz, DMSO-d_6): δ 7.75 (m, 1H), 3.12 – 2.97 (m, 2H), 2.88 (d, *J* = 5.1 Hz, 1H), 1.83 (m, 1H), 1.38 (m, 2H), 1.24 (m, 12H), 0.87 (m, 6H), 0.77 (d, *J* = 6.8 Hz, 3H). The amine's signals (NH_2) are very broad and cannot be distinguished in the spectrum. ^{13}C NMR (126 MHz, DMSO-d_6): δ 174.2 (C=O), 60.0 (CH), 38.2 (CH_2), 31.6 (CH_2), 31.2 (CH), 29.2 (CH_2), 28.9 (CH_2), 28.7 (CH_2), 28.6 (CH_2), 26.4 (CH_2), 22.1 (CH_2), 19.5 (CH_3), 17.1 (CH_3), 13.9 (CH_3).

*(S)-4-((3-methyl-1-(nonylamino)-1-oxobutan-2-yl)amino)-4-oxobutanoic acid (**1**):* Powdered K_2CO_3 (7.4 g, 53.5 mmol, 3.8 eq.) was added to a solution of amine **2** (3.54 g, 14.6 mmol) in THF (290 mL) at 0 °C under N_2 with and stirred for 15 minutes. Then a solution of succinic anhydride (2.92 g, 29.2 mmol, 2.0 eq.) in THF (100 mL) was added dropwise and the mixture was stirred vigorously for 16 h at room temperature. After this time, the solution was concentrated under reduced pressure and the crude residue was dissolved in water (200 mL). Finally, concentrated hydrochloric acid was added dropwise at 0 °C until the formation of a white precipitate at pH = 3. The white solid obtained was filtered under vacuum, and the residue was washed with water (300 mL). The compound was dried under reduced pressure at 50 °C to yield **1** (4.86 g, 14.2 mmol, 97%) as a white solid. ^{1}H NMR (500 MHz, DMSO-d_6): δ 11.99 (br s, 1H), 7.80 (m, 2H), 4.07 (t, *J* = 7.9 Hz, 1H), 3.15 – 2.90 (m, 2H), 2.47 – 2.32 (m, 4H), 1.92 (m, 1H), 1.36 (m, 2H), 1.23 (m, 12H), 0.85 (t, *J* = 6.7 Hz, 3H), 0.81 (d, overlapped, *J* = 5.3 Hz, 6H). ^{13}C NMR (126 MHz, DMSO-d_6): δ 174.3 (C=O), 171.5 (C=O), 171.2 (C=O), 58.3 (CH), 38.8 (CH_2), 31.7 (CH_2), 30.9 (CH_2), 30.4 (CH_2), 29.8 (CH), 29.4 (CH_2), 29.4 (CH_2), 29.1 (CH_2), 29.1 (CH_2), 26.8 (CH_2), 22.5 (CH_2), 19.6 (CH_3), 18.6 (CH_3), 14.4 (CH_3). HRMS (ESI-TOF): *m/z* calcd. for $[C_{18}H_{35}N_2O_4]^+$: 343.2597; found: 343.2591 [*M* + H]$^+$ (Δ = 1.7 ppm).

Macroscopic gel preparation

In a typical experiment, 5 mg of compound **1** and 1 mL of solvent were introduced into a cylindrical screw-capped glass vial (8 mL, diameter = 1.5 cm). The system was sonicated to obtain a homogeneous suspension and the vial was heated (hot air at 250 ºC from a heat gun) until a clear solution was obtained. Then, the vial was introduced into a thermostatic bath at 25 ºC. After 10-20 minutes, the formation of the gel was assessed by turning the vial upside down (all the solvent remains entrapped).

Nanogel particles preparation

On a representative example, a suspension of 7.3 µmol of compound **1** in 1 mL toluene in a screw-capped vial (4 mL, diameter = 1.3 cm) was heated (heat gun, 250 ºC) until complete solution. After cooling down (thermostatic bath, 25 ºC), a gel was obtained. Then, solvent was removed under vacuum and the xerogel was hydrated in 2 mL of phosphate buffer saline (PBS, 10 mM, pH 7, filtered over a nylon 0.45 µm mesh filter) for 10 min. At this point, the system was ultrasonicated during *ca.* 10 minutes until a homogenous suspension was obtained, with a final pH of 6.4. Then, large particles were removed by centrifugation at 6.000 rpm for 60 min to give a clear solution of the nanogel particles.

Transmission Electron Microscopy (TEM, Cryo-TEM)

Transmission electron micrographs were taken on a JEOL 2100 microscope with thermionic gun LaB6 200 kV equipped with Gatan Orius high resolution CCD camera. TEM samples were prepared over Formvar/Carbon film on 200 mesh copper grids.
Gels: Fresh gels were applied directly onto a grid and expelled solvent was carefully removed by capillarity with paper. The grids were immediately stained with one drop of 1% aqueous phosphotungstic acid for 2 min and the liquid was subsequently removed by capillary action.
Nanogels: A drop of nanogels suspension was added over a grid and incubated for 2 min. Then, solvent was removed with filter paper by capillarity and a drop of OsO_4 0.1% was added. After 5 min, the staining solution was removed by capillarity and the grid was washed with a drop of miliQ water.
For Cryo-TEM technique, JEM-2200FS/CR transmission electron microscope (JEOL, Japan), equipped with an UltraScan 4000 SP (4008x4008 pixels) cooled slow-scan CCD camera (GATAN, UK) was used. A drop of the nanogel suspension was placed on the TEM grid and an automated vitrification robot Vitrobot™ was used to freeze the sample in liquid ethane.

Potentiometric titration

Potentiometric titrations to determine pKa of **1** were carried out at 25 ºC. An aqueous solution (0.5 mg mL^{-1}, 5 mL) of compound **1** in sodium hydroxide 0.1 M was titrated with vigorous stirring with a 0.1 M normalized solution of hydrochloric acid. The addition rate was 6 mL h^{-1} and pH was monitored every 10 s (in a S220 Seven Compact pHmeter, Mettler Toledo). pKa was calculated by fitting experimental data to calculated titration curves with the program HYPERQUAD.[66]

Determinaton of the critical aggregation concentration (cac)

The critical aggregation concentration of compound **1** at pH 1 was determined using pyrene fluorescence changes (peak I/peak III ratio). A series of solutions of gelator **1** at different concentrations (0-500 µg mL^{-1}) and pyrene (1 µg mL^{-1}) were prepared in 0.1M aqueous NH_4OH. Then, the samples were acidified to pH 1 with 2 M H_2SO_4 (promoting aggregation) and fluorescence was recorded (λ_{ex} = 334 nm).

Nile Red loading

A macroscopic gel of compound **1** was prepared using 1 mL 10 µM Nile Red solution in toluene. Then, the procedure reported above was carried out to obtain nanoparticles.

Dynamic light scattering

Size measurements of nanogel particles were performed using dynamic light scattering (DLS) with a Zetasizer Nano ZS (Malvern). Analyses were carried out with a He-Ne laser (633 nm) at a fixed scattering angle of 173º. Automatic optimization of beam focusing and attenuation was applied for each sample. When measurements were performed at 25 ºC, nanogels suspensions were introduced in 3 mL disposable PMMA cuvettes (10 mm optical path length). Otherwise, samples were placed in 3 mL optical glass cuvettes (10 mm optical path, Hellma Analytics). In the latter case, 5 min of sample stabilization was used each time temperature was changed. Particle size was reported as the average of three measurements.

Z-potential

Z-potential measurements were performed at 25 ºC using Laser Doppler Micro-electrophoresis with a Zetasizer Nano ZS (Malvern). 1 mL of nanogels suspension was measured in disposable folded capillary zeta cells (Malvern, DTS1070). Z-potential is reported as the average of six measures per sample of five different samples.

Single angle static light scattering

Single angle static light scattering (SALS) measuraments were performed with a Zetasizer Nano ZS (Malvern). Samples were introduced in 3 mL optical glass cuvettes (10 mm optical path, Hellma Analytics) and toluene was used as a standard. The refractive index increment (*dn/dC*) for the nanogel particles was set to 0.063 mL g^{-1}, according to results obtained in a AF2000 system (Postnova Analytics) using the refractive index detector in batch mode. The use of SALS requires the simplification of considering isotropic scattering, using value of 1 for $P(\theta)$ in equation *(2).* This assumption is calculated to generate an error of 60% in M_w value for particles with diameter of 200 nm (Zetasizer Nano application note *"Molecular weight measurements with the Zetasizer Nano system"*).
To assess the reliability of SALS in the determination of nanoparticles M_w, measurements were carried out for a standard of monodisperse polystyrene latex nanoparticles (diameter = 100 nm). Using a value of *dn/dc* of 0.159 mL g^{-1} [67] the M_w of PS nanoparticles was calculated to be $6.1\ 10^5 \pm 2\ 10^5$ kDa. This value is in reasonable agreement with that obtained

considering solid-like particles with a density of 1.04 g mL^{-1} and a diameter of 100 nm, which results in M_w = 3.3 10^5 kDa (see ESI).

Gelator quantification using NMR ERETIC

The concentration of **1** in a nanogel suspension was quantified using ^{1}H NMR (Bruker Avance III HD spectrometer 400 MHz) after lyophilization and solubilization of **1** in a 6:1 mixture of $CDCl_3$/Hexafluoroisopropanol. A calibrated electronic signal (ERETIC) at δ 11.0 ppm was used for this purpose.

Fluorescence spectroscopy

Fluorescence measurements were carried out in a JASCO FP-8300 spectrofluorometer equipped with a Peltier accessory ETC-815 at 25 ºC. Samples were placed in 3 mL disposable PMMA cuvettes (10 mm optical path length).

Conclusions

Merging the interest in polymeric nanogels as nanocarriers and in molecular gels as new soft materials, the preparation of molecular nanogel particles by self-assembly of a low molecular weight compound is reported. Compound **1** forms macroscopic gels in water and a variety of organic solvents. Nanosized particles in concentrations as high as *ca.* 2 mM were prepared reproducibly by sonication of a xerogel of **1** in aqueous media. Electron microscopy reveals spherical particles that would correspond to the initial stages of the aggregation into fibers. SALS indicates that the nanogels are composed mainly by water, as the analogous macroscopic material. The described nanogels seem to constitute an intermediate state between free molecules and self-assembled fibrillar networks. The particles show good temporal and thermal stability and present accessible hydrophobic domains that entrap Nile Red. In the so-called race for drug delivery, the use of polymeric nanogels presents challenges associated to stimuli-triggered release, biodegradation, and batch-to-batch reproducibility in the preparation of polymers.[68] The particles described here should present intrinsic advantages compared to polymeric nanogels, such as stimuli-triggered disassembly and improved biodegradability due to their molecular nature. Further work will be carried out in the next future to assess the feasibility of loading different bioactive substrates in the particles and their use as nanocarriers in cells. It has to be considered that the extensive library of molecular gelators available paves the way to the preparation of molecular nanogels with tailored properties, such as stimuli responsiveness or the presence of the desired functional groups in their structure.

Conflicts of interest

There are no conflicts to declare.

Acknowledgements

Ministerio de Economía y Competitividad of Spain (grant CTQ2015-71004-R) and Universitat Jaume I (grant P1.1B2015-76) are thanked for financial support. A.T.-M. thanks Ministerio de Educación, Cultura y Deporte of Spain for a FPU fellowship (FPU14/05974). Technical support from SCIC of University Jaume I and Dr. David Gil (CIC bioGUNE) for his assistance in cryo-TEM measurements are acknowledged.

Notes and references

1. K. Öztürk-Atar, H. Eroğlu and S. Çalış, *J. Drug Target.*, 2018, **26**, 633-642.
2. V. P. Torchilin, *Nat. Rev. Drug Discov.*, 2005, **4**, 145-160.
3. B. Aryasomayajula, G. Salzano and V. P. Torchilin, *Methods Mol. Biol.*, 2017, **1530**, 41-61.
4. M. Geszke-Moritz and M. Moritz, *Mater. Sci. Eng., C*, 2016, **68**, 982-994.
5. B. L. Banik, P. Fattahi and J. L. Brown, *WIREs. Nanomed. Nanobi.*, 2016, **8**, 271-299.
6. A. P. Sherje, M. Jadhav, B. R. Dravyakar and D. Kadam, *Int. J. Pharm.*, 2018, **548**, 707-720.
7. M. Elsabahy, G. S. Heo, S. M. Lim, G. Sun and K. L. Wooley, *Chem. Rev.*, 2015, **115**, 10967-11011.
8. S. Wang, P. Huang and X. Chen, *ACS Nano*, 2016, **10**, 2991-2994.
9. D. Bobo, K. J. Robinson, J. Islam, K. J. Thurecht and S. R. Corrie, *Pharm. Res.*, 2016, **33**, 2373-2387.
10. M. Hamidi, A. Azadi and P. Rafiei, *Adv. Drug Deliv. Rev.*, 2008, **60**, 1638-1649.
11. J. K. Oh, R. Drumright, D. J. Siegwart and K. Matyjaszewski, *Prog. Polym. Sci.*, 2008, **33**, 448-477.
12. A. V. Kabanov and S. V. Vinogradov, *Angew. Chem. Int. Ed.*, 2009, **48**, 5418-5429.
13. R. T. Chacko, J. Ventura, J. Zhuang and S. Thayumanavan, *Adv. Drug Deliv. Rev.*, 2012, **64**, 836-851.
14. K. S. Soni, S. S. Desale and T. K. Bronich, *J. Control. Release*, 2016, **240**, 109-126.
15. I. Neamtu, A. G. Rusu, A. Diaconu, L. E. Nita and A. P. Chiriac, *Drug Deliv.*, 2017, **24**, 539-557.
16. J. Estelrich, M. Quesada-Pérez, J. Forcada and J. Callejas-Fernández, *Soft Nanoparticles for Biomedical Applications*, Royal Society of Chemistry, 2014.
17. A. Vashist, A. K. Kaushik, S. Ahmad and M. Nair, *Nanogels for Biomedical Applications*, Royal Society of Chemistry, 2017.
18. K. Raemdonck, J. Demeester and S. De Smedt, *Soft Matter*, 2009, **5**, 707-715.
19. L. Zha, B. Banik and F. Alexis, *Soft Matter*, 2011, **7**, 5908-5916.
20. J. Ramos, A. Imaz, J. Callejas-Fernández, L. Barbosa-Barros, J. Estelrich, M. Quesada-Pérez and J. Forcada, *Soft Matter*, 2011, **7**, 5067-5082.
21. C. C. Lin and A. T. Metters, *Adv. Drug Deliv. Rev.*, 2006, **58**, 1379-1408.
22. Q. Li, Z. Ning, J. Ren and W. Liao, *Curr. Med. Chem.*, 2018, **25**, 963-981.
23. S. Khoee and H. Asadi, *Nanogels: Chemical Approaches to Preparation. In Encyclopedia of Biomedical Polymers and Polymeric Biomaterials.*, Taylor and Francis, 2016.
24. K. Landfester, A. Musyanovych and V. Mailänder, *J. Polym. Sci. A*, 2010, **48**, 493-515.

25. S. Vinogradov, E. Batrakova and A. Kabanov, *Colloids Surf. B*, 1999, **16**, 291-304.
26. R. Lupitskyy and S. Minko, *Soft Matter*, 2010, **6**, 4396-4402.
27. X. Zhang, S. Malhotra, M. Molina and R. Haag, *Chem. Soc. Rev.*, 2015, **44**, 1948-1973.
28. A. Rösler, G. W. M. Vandermeulen and H.-A. Klok, *Adv. Drug Deliv. Rev.*, 2001, **53**, 95-108.
29. K. Akiyoshi, S. Deguchi, H. Tajima, T. Nishikawa and J. Sunamoto, *Macromolecules*, 1997, **30**, 857-861.
30. H. V. P. Thelu, S. K. Albert, M. Golla, N. Krishnan, D. Ram, S. M. Srinivasula and R. Varghese, *Nanoscale*, 2018, **10**, 222-230.
31. P. Terech and R. G. Weiss, *Chem. Rev.*, 1997, **97**, 3133-3159.
32. L. A. Estroff and A. D. Hamilton, *Chem. Rev.*, 2004, **104**, 1201-1217.
33. A. R. Hirst, B. Escuder, J. F. Miravet and D. K. Smith, *Angew. Chem. Int. Ed.*, 2008, **47**, 8002-8018.
34. S. Banerjee, R. K. Das and U. Maitra, *J. Mater. Chem.*, 2009, **19**, 6649-6687.
35. J. W. Steed, *Chem. Commun.*, 2011, **47**, 1379-1383.
36. X. Du, J. Zhou, J. Shi and B. Xu, *Chem. Rev.*, 2015, **115**, 13165-13307.
37. E. R. Draper and D. J. Adams, *Chem*, 2017, **3**, 390-410.
38. M. D. Segarra-Maset, V. J. Nebot, J. F. Miravet and B. Escuder, *Chem. Soc. Rev.*, 2013, **42**, 7086-7098.
39. C. Felip-León, R. Cejudo-Marín, M. Peris, F. Galindo and J. F. Miravet, *Langmuir*, 2017, **33**, 10322-10328.
40. V. J. Nebot, J. Armengol, J. Smets, S. F. Prieto, B. Escuder and J. F. Miravet, *Chem. Eur. J.*, 2012, **18**, 4063-4072.
41. M. Fontanillo, C. A. Angulo-Pachón, B. Escuder and J. F. Miravet, *J. Colloid Interface Sci.*, 2013, **412**, 65-71.
42. C. A. Angulo-Pachón and J. F. Miravet, *Chem. Commun.*, 2016, **52**, 5398-5401.
43. C. Tang, A. M. Smith, R. F. Collins, R. V. Ulijn and A. Saiani, *Langmuir*, 2009, **25**, 9447-9453.
44. L. Chen, S. Revel, K. Morris, L. C. Serpell and D. J. Adams, *Langmuir*, 2010, **26**, 13466-13471.
45. M. Tena-Solsona, B. Escuder, J. F. Miravet, V. Casttelleto, I. W. Hamley and A. Dehsorkhi, *Chem. Mater.*, 2015, **27**, 3358-3365.
46. X. Yan, Y. Cui, W. Qi, Y. Su, Y. Yang, Q. He and J. Li, *Small*, 2008, **4**, 1687-1693.
47. S. Akoka, L. Barantin and M. Trierweiler, *Anal. Chem.*, 1999, **71**, 2554-2557.
48. M. I. Burguete, F. Galindo, E. García-Verdugo, N. Karbass and S. V. Luis, *Chem. Commun.*, 2007, **0**, 3086-3088.
49. E. D. Sone, S. Weiner and L. Addadi, *Journal of Structural Biology*, 2007, **158**, 428-444.
50. C. Wu and S. Zhou, *J. Macromol. Sci., Phys.*, 1997, **36**, 345-355.
51. R. Pelton, *Macromol. Symp.*, 2004, **207**, 57-65.
52. N. Morimoto, S. Hirano, H. Takahashi, S. Loethen, D. H. Thompson and K. Akiyoshi, *Biomacromolecules*, 2013, **14**, 56-63.
53. S. Islam, D. L. Inglefield and O. D. Velev, *Soft Matter*, 2018, **14**, 2118-2130.
54. B. H. Zimm, *J. Chem. Phys.*, 1948, **16**, 1093-1099.
55. N. Zębacz, S. A. Wieczorek, T. Kalwarczyk, M. Fiałkowski and R. Hołyst, *Soft Matter*, 2011, **7**, 7181-7186.
56. S. Peng and C. Wu, *Macromolecules*, 2001, **34**, 568-571.
57. Y. Sekine, H. Endo, H. Iwase, S. Takeda, S. A. Mukai, H. Fukazawa, K. C. Littrell, Y. Sasaki and K. Akiyoshi, *J. Phys. Chem. B*, 2016, **120**, 11996-12002.
58. Q. Ying and B. Chu, *Macromolecules*, 1987, **20**, 362-366.
59. A. Aggeli, I. A. Nyrkova, M. Bell, R. Harding, L. Carrick, T. C. B. McLeish, A. N. Semenov and N. Boden, *Proc. Natl. Acad. Sci. USA*, 2001, **98**, 11857-11862.
60. X. Huang, P. Terech, S. R. Raghavan and R. G. Weiss, *J. Am. Chem. Soc.*, 2005, **127**, 4336-4344.
61. M. A. Rogers, X. Liu, V. A. Mallia and R. G. Weiss, *CrystEngComm*, 2015, **17**, 8085-8092.
62. C. D. Jones, S. R. Kennedy, M. Walker, D. S. Yufit and J. W. Steed, *Chem*, 2017, **3**, 603-628.
63. J. Stachurski and M. Michałek, *J. Colloid Interface Sci.*, 1996, **184**, 433-436.
64. K. A. Fletcher, I. A. Storey, A. E. Hendricks, S. Pandey and S. Pandey, *Green Chemistry*, 2001, **3**, 210-215.
65. J. Becerril, M. Bolte, M. I. Burguete, F. Galindo, E. García-España, S. V. Luis and J. F. Miravet, *J. Am. Chem. Soc.*, 2003, **125**, 6677-6686.
66. L. Alderighi, P. Gans, A. Ienco, D. Peters, A. Sabatini and A. Vacca, *Coord. Chem. Rev.*, 1999, **184**, 311-318.
67. J. Jacobs, A. Byrne, N. Gathergood, T. E. Keyes, J. P. A. Heuts and A. Heise, *Macromolecules*, 2014, **47**, 7303-7310.
68. S. V. Vinogradov, *Nanomedicine*, 2010, **5**, 165-168.